

MRI image reconstruction research based on discrete shearlet transform

Xu Hong

School of Information Science and Engineering, Hunan International Economics University,
Changsha, 410205, China
E-mail: matlab_bysj@126.com

Abstract: The two-dimensional wavelet transform for magnetic resonance imaging (MRI) does not represent sparsely curve singularity characteristics, it can only capture the limited direction information. In order to solve this problem, a new method for compressed sensing MRI (CS-MRI) is presented based on discrete shearlet transform in this paper. Frequency coefficients can be got at all scales and in all directions after discrete shearlet transform of MRI image. Then orthogonal matching pursuit algorithm is adopted to recover the sparsing coefficients. Finally, the reconstructed image is gotten by inverse shearlet transform. Experimental results show that compared with wavelet transform, discrete shearlet transform for CS-MRI improves quality of reconstructed image and preserves more information about texture and edge.

Keywords: discrete shearlet transform, compressed sensing (CS), MRI image's reconstruction, sparse expression, feature extraction

1. INTRODUCTION

The traditional signal sampling process must follow the Nyquist sampling frequency, which will undoubtedly increase the sample volume, it is a huge challenge to transport and store. The compressed sensing theory is as a new signal acquisition theory[1,2], as long as the signal is compressible or is sparse in a transform domain, it can be optimized by solving related problems, the original signal is restored by random sampling transform coefficient. Magnetic resonance imaging is an important means of clinical imaging, MRI image has a sparse representation in a transform domain (such as spatial finite difference and wavelet transform domain, etc.)[3-6]. In order to meet the compressed sensing sparse image reconstruction requirement, a number of scholars' researches show that the theory of MRI images compressed sensing reconstruction is an important field of application [7-10].

In compressed sensing, the sparsity of the reconstructed image quality has a significant impact, the current traditional two-dimensional wavelet transform base is usually used to sparse sparse MRI images. However, two-dimensional wavelet decomposition are only horizontal, vertical, and diagonal direction, and the transform filter is isotropic, the singular point feature in image can preferably be sparsed, a characteristic curve of singularities can not be represented in the sparsity [11]. MRI images often contain a lot of curves and

edges, and therefore two-dimensional wavelet transform can not provide the best representation of the image.

Shear waves (Shearlet) is the latest development of multi-scale geometric analysis, after an synthesized and expansion affine system is used by Guo et al [12,13], multi-dimensional functions are constructed close to the optimal representation, it has a more simple math structure, in the image represents, there are multi-resolution, non-linear approximation and optimal directionality and so on. The shear waves has excellent characteristics, it provides a new research ideas for solving difficult problems in image processing.

Based on the above ideas, this paper analyzes the MRI image signal sparse characteristics in shear wave transformation, for the first time, discrete shear waves transform is used to sparse MRI image processing, and orthogonal matching pursuit algorithm is used as a compressed sensing reconstruction algorithm, the compressed sensing MRI image reconstruction is achieved.

2. Shearlet principle

2.1. Continuous shear wave transformation

Shear wave transformation theory is based on the synthesis of wavelet theory [12,13]. Synthetic wavelet theory provides an effective method for

geometry multiscale analysis through affine systems. When the dimension is 2, the affine system with a synthetic expansion is as follows:

$$\Psi_{AB}(\psi) = \{\psi_{j,k,l}(x) = |\det A|^{j/2} \psi(B^l A^j x - k)\} \quad (1)$$

Which meet $j, l \in \mathbb{Z}$, $k \in \mathbb{Z}^2$, $\psi \in L^2(\mathbb{S}^2)$. A and B are 2×2 invertible matrices, $|\det B| = 1$. If $\Psi_{AB}(\psi)$ meets tight frame structure, its elements are called synthetic wavelets. Among them, matrix A^j is associated with the scale transformation, B^l is associated with the constant holding area geometric transformation. Shear wave transform is a special case of the synthesis wavelet, if $\psi \in L^2(\mathbb{S}^2)$ satisfies the following conditions:

$$1) \hat{\psi}(\xi) = \psi(\xi_1, \xi_2) = \psi_1(\xi_1) \psi_2\left(\frac{\xi_2}{\xi_1}\right), \text{ which } \hat{\psi} \text{ is}$$

ψ 's Fourier transform.

$$2) \psi_1 \text{ continuous wavelet, } \hat{\psi}_1 \in C^\infty(\mathbb{S}), \text{ supp } \hat{\psi}_1 \subset [-2, -1/2] \cup [1/2, 2].$$

3) $\hat{\psi}_2 \in C^\infty(\mathbb{S})$ and $\text{supp } \hat{\psi}_2 \subset [-1, 1]$, in the interval $(-1, 1)$, $\psi_2 > 0$ and $\|\psi_2\| = 1$, the following

system is generated by the ψ , $A_a = \begin{pmatrix} a & 0 \\ 0 & \sqrt{a} \end{pmatrix}$ and

$$B_s = \begin{pmatrix} 1 & s \\ 0 & 1 \end{pmatrix}.$$

$$\psi_{ast}(x) = \{a^{-\frac{3}{4}} \psi(A_a^{-1} B_s^{-1}(x-t)), \quad a \in \mathbb{S}^+, s \in \mathbb{S}, t \in \mathbb{S}^2\} \quad (2)$$

$$Sf(a, s, t) = \langle f, \psi_{ast} \rangle \quad (3)$$

Which is continuous shear-wave system, and $\psi_{ast}(x)$ is called continuous shear waves.

2.2. Discrete shear wave transformation

The scale parameters and shear parameters are discretized, and discrete shear wave transformation is enabled. Localization properties of discrete shear wave is very good, supporting regional basis functions satisfy the parabolic scaling, the singularity of the characteristic function can be accurately described with changes in scale[14]. Usually, shear matrix B and anisotropic expansion of matrix A are taken.

$$A = \begin{pmatrix} 4 & 0 \\ 0 & 2 \end{pmatrix}, \quad B = \begin{pmatrix} 1 & 1 \\ 0 & 1 \end{pmatrix} \quad (4)$$

Function of discrete shear waves is as follows:

$$\psi_{j,l,k}^{(0)}(x) = 2^{\frac{3j}{2}} \psi(B^l A^j x - k) \quad (5)$$

$$\text{Which } \hat{\psi}^{(0)}(\xi) = \psi^{(0)}(\xi_1, \xi_2) = \psi_1(\xi_1) \psi_2\left(\frac{\xi_2}{\xi_1}\right),$$

$$\hat{\psi}_1, \hat{\psi}_2 \in C^\infty(\mathbb{S}), \text{ supp } \hat{\psi}_1 \subset \left[-\frac{1}{2}, -\frac{1}{16}\right] \cup \left[\frac{1}{16}, \frac{1}{2}\right],$$

$$\text{supp } \hat{\psi}_2 \subset [-1, 1].$$

If it is assumed

$$\sum_{j \geq 0} |\hat{\psi}_1(2^{-2j} \omega)|^2 = 1 \text{ for } |\omega| \geq \frac{1}{8} \quad (6)$$

If $j \geq 0$

$$\sum_{\ell=-2^j}^{2^j-1} |\hat{\psi}_2(2^j \omega - \ell)|^2 = 1 \text{ for } |\omega| \leq 1 \quad (7)$$

From the above assuming, function $\hat{\psi}_{j,l,k}^{(0)}$ ($j \geq 0, -2^j \leq \ell \leq 2^j - 1, k \in \mathbb{S}^2$) constitutes a split shear waves in the frequency domain, which is $D_0 = \{(\xi_1, \xi_2) : |\xi_1| \geq \frac{1}{8}, |\frac{\xi_2}{\xi_1}| \leq 1\}$, it is shown in Figure 1 (a). Each element $\hat{\psi}_{j,l,k}^{(0)}$ is supported on the trapezoid, the approximate size is $2^{2j} \times 2^j$, The direction slope is $l2^{-j}$ straight line, it is shown in Figure 1 (b).

Similarly understood, a function $\hat{\psi}_{j,l,k}^{(1)}(x)$ can be constructed, it satisfies

$$\{\hat{\psi}_{j,l,k}^{(1)} : j \geq 0, -2^j < l < 2^j - 1, k \in \mathbb{S}^2\},$$

Which shear wave is split in frequency domain, it is $D_1 = \{(\xi_1, \xi_2) : |\xi_2| \geq \frac{1}{8}, |\frac{\xi_1}{\xi_2}| \leq 1\}$, it is shown in Figure 1 (a). The appropriate $\varphi \in L^2(\mathbb{S}^2)$ is selected to meet $\{\varphi_k(x) = \varphi(x - k) : k \in \mathbb{S}^2\}$, which is $L^2\left([-\frac{1}{16}, \frac{1}{16}]^2\right)$ tight frame. Thus, a collection $\{\varphi_k, \psi_{j,l,k}^{(d)} : j \geq 0, -2^j < l < 2^j - 1, k \in \mathbb{S}^2, d = 0, 1\}$ of shear waves is $L^2(\mathbb{S}^2)$ tight frame.

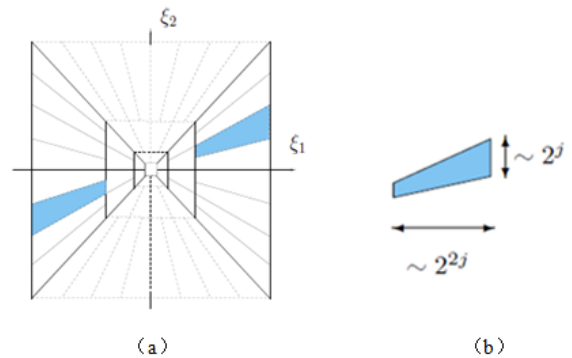


Fig. 1. Shear wave frequency domain subdivision map and cross-sectional area geometry [12]
 ((a) shear waves frequency domain subdivision graph; (b) shear waves frequency domain support)

In summary, shear wave has the following good properties: (1) very good localization characteristics; (2) to satisfy the parabolic scaling characteristics; (3) there is good directional sensitivity; (4) shear waves can represent a rich direction, and it is close to the optimal image information on a variety of scales and directions.

3. Image reconstruction based on compressed sensing

Compressed sensing theory is a new theoretical framework, a sampling is combined with compression process. If the signal A is compressible in orthogonal basis or on a tight frame B, the signal nonlinear reconstruction is made from the relatively small measurement, and it is precise or approximate recovery[15].

Specific steps are as follows:

1) sparse signals. Sparse transform coefficient vector $a = \psi^T x$ is obtained, which is only K non-zero transform coefficients ($K \ll N$).

2) The projection matrix $\phi \in R^{M \times N}$ ($M < N$) is used to project signals to obtain the observed values $y = \phi x = \phi \psi a = \Theta a$ of the signal. Theory shows that if Θ meets the limited equidistant (RIP) nature [16], the observation y is used to reconstruct the signal x.

3) Reconstructed signal can be expressed as solving the problem l_0 norm, it is expressed as $\min_x \|\psi^T x\|_0$ s.t. $y = \phi x$, Minimal solution of non-zero element number is looked from transform coefficient, which x solution is most sparse.

The problem is a NP-Hard problem, its solving approach is not unique, the most widely application and the most representative Orthogonal Matching (OMP) algorithm are used[17], the MRI image compression is sampled and reconstructed.

4. Compressed sensing MRI image reconstruction based on discrete shear waves

Sparse representation of the signal is compressed sensing priori conditions. In the MRI image reconstruction based on compressed sensing, the two-dimensional wavelet transform is commonly used as a sparse group, while the wavelet transform image can not give the optimal representation to high anisotropic edge and texture direction information, these affects the quality of the reconstruction. There are multi-directional and anisotropic strengths in

discrete shear wave, the discrete shear wave transform is selected as MRI image sparse transformation in this paper.

Discrete shear waves transform of MRI images can be divided into two steps in the frequency domain, which are namely multi-scale subdivision and localized direction. The image field is developed and represented in the form of a finite group \aleph^2 , a discrete MRI image $f \in l^2(\aleph_n^2)$ is given, and f is decomposed into L layer[14].

Step 1. Multiscale subdivision. Symmlet wavelet basis is used as a mother function, discrete domain image f is decomposed, low frequency coefficients f_a^j and high frequency coefficients f_d^j are obtained under various scales, where j is the decomposed scales.

Step 2. Localized Direction. In order to obtain high-frequency components in different directions, in each scale factor, the high-frequency is split under the band direction and scale changes of tapered function, it is as shown in Figure 1 (a). The above steps is repeated until $j = L$ stops. The two scales ($L = 2$) discrete shear waves flow chart shows in Figure 2.

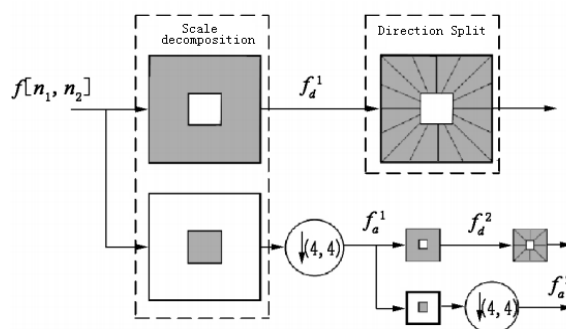


Fig.2. Discrete shear waves flow chart

Among them, the scale vector *scale* can be set as $scale = [s_1 \ s_2 \ \dots \ s_L]$, the support size of the scale j is $2^{-(L-s_j)} \times 2^{-(L-j)}$ in the horizontal cone direction, the support size of the scale j is $2^{-(L-j)} \times 2^{-(L-s_j)}$ in the vertical cone direction. The direction vector *ndir* is set as $ndir = [n_1 \ n_2 \ \dots \ n_L]$, scale j has both $2 \times 2^{n_j} + 1$ directions in horizontal cone and vertical cone. Figure 3 is MRI images exploded view, when $L = 2$, $scale = [2 \ 3]$, $ndir = [1 \ 1]$, there are both five directions in the horizontal cone and vertical cone.

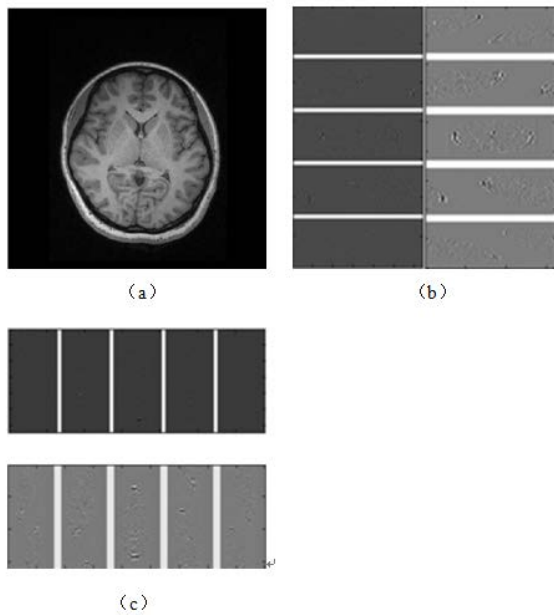


Fig.3. Two layer exploded view of MRI images in discrete shear waves
 ((a) MRI image; (b) decomposition level is 2, the coefficient of shear wave in horizontal cone direction; (c) decomposition level is 2, the coefficient of shear wave in vertical cone direction)

In summary, based on discrete shear waves, compressed sensing MRI reconstruction algorithm is described as follows:

- 1) MRI images are decomposed in discrete shear wave, shear coefficient is obtained in each scale, directional sub bands.
- 2) The sampling rate is set, the measurement matrix is constructed.
- 3) wave frequency subbands of discrete shear transform coefficient were measured, decomposition coefficient is retained for the low frequency approximation subband. Thus one can reduce effectively the amount of data which is required for image reconstruction, other hand, it effectively improves the quality of the reconstructed image.
- 4) OMP algorithm is used as a compressed sensing reconstruction algorithm, sparse coefficient is recovered after treatment.
- 5) By shear-wave inverse transform, the approximation image is restored after reconstruction, and the reconstructed image is finally gotten.

5. Experimental results and analysis

5.1. Objective evaluation methods of the image reconstruction quality

In order to objectively evaluate the quality of image reconstruction, three kinds of objective assessment methods are used:

- 1) MSE (Mean Square Error, MSE). Let the size of the original MRI image be $M \times N$, where the

original image is represented by f , image reconstruction is represented by \hat{f} , the MSE is defined as: $MSE = \frac{1}{MN} \|f - \hat{f}\|^2$

- 2) PSNR (Peak Signal-to-Noise Ratio, PSNR) is defined as follows: $PSNR = 10 \lg \frac{M \times N}{MSE}$ [18,19]

- 3) structural similarity (Structural Similarity, SSIM) is a measure of the similarity of two images, it is a new index, the more large the value, the better the value, its maximum value is 1. The original image is represented by f , image reconstruction is represented by \hat{f} , SSIM is defined as:

$$SSIM(f, \hat{f}) = [l(f, \hat{f})]^\gamma \cdot [c(f, \hat{f})]^\eta \cdot [s(f, \hat{f})]^\mu$$

Which γ, η, μ is used, $\gamma, \eta, \mu \in (0, 1)$, respectively, to adjust the brightness, the contrast and the heavy right of structural information, $l(f, \hat{f})$ is brightness comparison function, $c(f, \hat{f})$ is for contrast comparison function, $s(f, \hat{f})$ is for structure comparison function, their definitions are

$$l(f, \hat{f}) = \left(\frac{2\mu_f \mu_{\hat{f}} + c_1}{\mu_f^2 + \mu_{\hat{f}}^2 + c_1} \right), \quad c(f, \hat{f}) = \left(\frac{2\delta_f \delta_{\hat{f}} + c_2}{\delta_f^2 + \delta_{\hat{f}}^2 + c_2} \right)$$

$$\text{and } s(f, \hat{f}) = \left(\frac{\delta_{\hat{f}\hat{f}} + c_3}{\delta_f \delta_{\hat{f}} + c_3} \right). \text{ Among them, } \mu_f, \mu_{\hat{f}}$$

is respectively the brightness mean of f, \hat{f} , $\delta_f, \delta_{\hat{f}}$ is respectively the standard deviation of f, \hat{f} , $\delta_{\hat{f}\hat{f}}$ is covariance, c_1, c_2, c_3 are generated by adding a constant, when the denominator is close to zero in order to prevent instability.

5.2. Experimental Analysis

256×256 brain MRI is selected to perform experiments in this article, compressed sensing image reconstruction algorithm OMP is used, the sparsity of the discrete shear waves is analyzed, the advantages of MRI compressed sensing reconstruction are tested based on discrete shear wave. In this paper, the discrete wavelet transform and shear wave transformation are as sparse transform, the reconstruction quality of MRI images were compared, and the image reconstruction quality effects of two type transformations are analyzed at different sampling rate. After a comparative analysis, $L = 5$, $scale = [2 \ 2 \ 3 \ 3 \ 4]$ are selected as decomposition scale.

5.2.1 Sparsity analysis of discrete shear wave

To test the shear wave sparsity, the shear wave transformation is done to test image, the absolute

value of the larger shear wave coefficients are retained only part, while other factors are set to 0, the retention percentage was 30%, 15%, 4% and 1%, then compressed sensing reconstruction process are done, and finally the reconstructed image is obtained in this part of shear wave inverse transform coefficients. Figure 3 is with sampling rate 0.5, the reconstructed image is obtained in the retention percentages of different coefficients, SSIM values and the PSNR of the reconstructed image are given in Table 1.

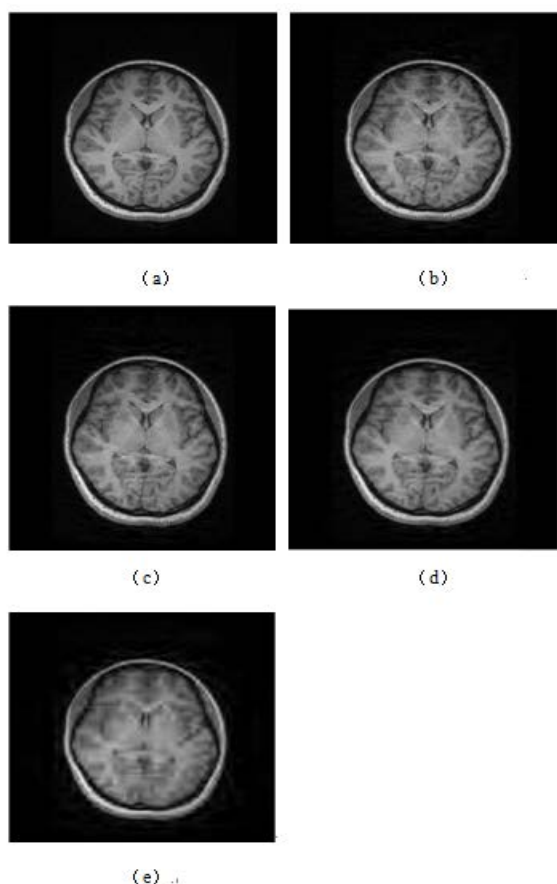


Fig.4. The reconstructed image in different retention rate coefficients ((a) of MRI picture; (b) 30% for the retention coefficient of the reconstructed image; (c) 15% for the retention coefficient of the reconstructed image; (d) 4% coefficient of retention reconstructed image; (e) 1% to preserve the image reconstruction coefficient)

Table 1. SSIM and PSNR values of the reconstructed image in reserved different percentage values of the coefficient

Retention percentage of coefficient	PSNR	SSIM
30%	39.13	0.8618
15%	39.96	0.8743
4%	39.27	0.8648
1%	34.85	0.7435

The foregoing analysis shows that when the retention factor are 30% and 15% coefficient, their reconstruction results are close, although retaining

only 1% of the coefficients, the reconstruction effect is variation, but the PSNR and SSIM values are obtained, and the reconstructed image can be accepted, therefore, there is good sparsity in shear waves transform, the accuracy of reconstruction can be ensured by compressed sensing.

5.2.2 The experimental comparison between wavelet transform and shearlet transform

Two-dimensional wavelet transform and shear wave conversion are done to test images respectively, some larger absolute coefficient are retained, while the other coefficients are set to 0, retention percentages are 16.73%, the images of the two sparse transform base are shown in Figure 4.

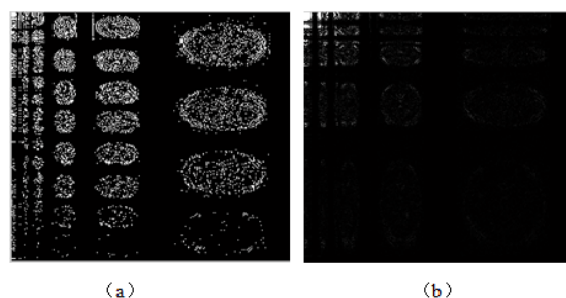


Fig.5. Sparse images based on two transform base ((a) shear wave discrete transform base; (b) the wavelet transform base)

When the sampling rate is 0.5, the reconstructed results are shown in Figure 6, the corresponding value of MSE, PSNR and SSIM are given in Table 2.

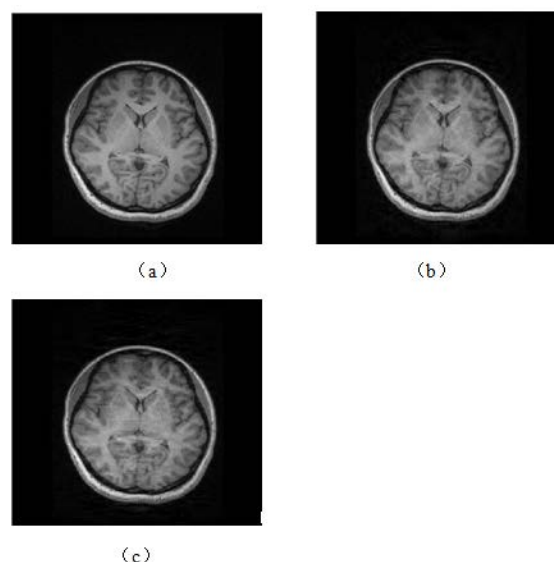


Fig.6. The results of experimental comparison between wavelet transform and shearlet transform ((a) for the MRI original; (b) wavelet-based image reconstruction; (c) reconstructed image based on shear waves)

Table 2. MSE, SSIM and PSNR values of reconstructed images based on wavelet transform and shearlet transform

	MSE	PSNR	SSIM
Wavelet base	1.9187e+006	33.46	0.8633
Shearlet base	1.8993e+006	39.53	0.8669

Meanwhile, in order to better illustrate the advantages of the reconstructed image edge detail based on the shearlet transform, Figure 7 shows the results of comparison of the edge map.

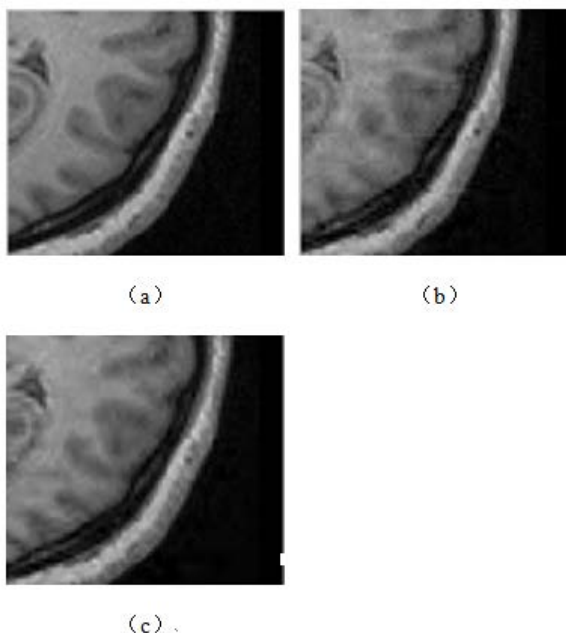


Fig.7. Reconstruction effect contrast of edge detail ((a) original edge portions; (b) edge portions of the reconstruction of wavelet-based; (c) edge portions of the shear-wave reconstruction based)

The foregoing analysis shows that the MRI reconstruction of compressed sensing is compared based on shearlet transform and wavelet transform, a smaller MSE value, higher PSNR, and SSIM are obtained based on shearlet transform, theoretically reconstruction result is better. Meanwhile, the reconstructed image is also significantly better visual effect, shear waves transform overcomes the non-sensitive detail of image edge in wavelet transform, there is an advantage for the reconstruction of edge details. Experiment shows that compressed sensing MRI reconstruction based on shear waves can improve the quality of image reconstruction.

5.2.3 Quality comparison of image reconstruction at different sampling rates

At different sampling rates, the quality of image reconstruction are compared and to analyzed between wavelet transform and discrete shearlet transform. At

different sampling rates, the corresponding SSIM values are shown in Figure 8, where the blue line represents the reconstruction based on wavelet transform, the red line represents reconstruction based on shearlet transform.

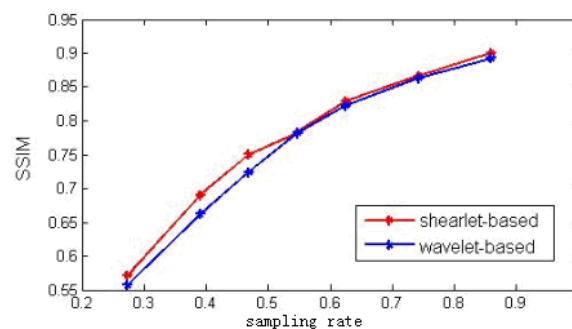


Fig.8. At different sampling rates, the SSIM values of the image reconstruction between two transform methods

Experimental results show that with the increase of the sampling rate, the reconstructed image structural similarity increases based on the two transform, the image quality is improvement. When the sampling rate is lower, SSIM value based on discrete shear waves is significantly higher than the reconstruction based on wavelet, the quality of its reconstruction has obvious advantages. When sampling rate is higher, the difference between the two methods is not obvious, the purpose of the compressed sensing is achieved by fewer low dimensional signal sample values to reconstruct the original high-dimensional signal, the sampling rate is typically selected to be less than 0.5, so The compressed sensing reconstruction based on discrete shearlet transform is superior to the conclusion based on wavelet reconstruction.

6. CONCLUSIONS AND OUTLOOK

Shear wave transform is a new multi-scale geometric analysis tool, we use multi-directional and anisotropic shear wave transformation, the advantages is that the curves and contours of the image can be well expressed, discrete shear waves are applied to MRI reconstruction in compressed sensing. Compared to the traditional two-dimensional wavelet transform and MRI reconstruction based on compressed sensing, this method has obvious advantages in this paper, the representation of MRI images can be more sparse, reconstruction is more accurate, and texture and edge information are retained more beneficially.

References

- [1] DONOHO D. Compressed Sensing[J]. IEEE Transactions on Information Theory, 2006, 52(4): 1289-1306.
- [2] CANDÈS E, TAO T. Near Optimal Signal Recovery from Random Projections: Universal Encoding Strategies[J]. IEEE Transactions on Information Theory, 2006, 52(12): 5406-5425.
- [3] A Jabbar Altaay, A., Bin Sahib, S., & Zamani, M. (2012). An Introduction to Image Steganography Techniques. Paper presented at the International Conference on Advanced Computer Science Applications and Technologies, Kuala Lumpur.
- [4] A Jabbar Altaay, A., Bin Sahib, S., & Zamani, M. (2013). Correlation Analysis of the Four Photo Themes in Five Layers Communications in Computer and Information Science (Vol. 398, pp. 211-222): Springer Berlin Heidelberg.
- [5] A Jabbar Altaay, A., Bin Sahib, S., & Zamani, M. (2013). Statistical Steganalysis of Four Photo Themes before Embedding. Paper presented at the International Conference on Advanced Computer Science Applications and Technologies, Sarawak.
- [6] A Jabbar Altaay, A., Bin Sahib, S., & Zamani, M. (2013). Pixel Correlation Behavior in Different Themes Communications in Computer and Information Science (Vol. 398, pp. 223-234): Springer Berlin Heidelberg.
- [7] M. Akcakaya, S. Nam, P. Hu et al, Compressed sensing with wavelet domain dependencies for coronary MRI: a retrospective study[J]. IEEE Transactions on Medical Imaging, 2011, 30(5): 1090–1099.
- [8] J. P. Haldar, D. Hernando, and Z.-P. Liang, Compressed Sensing MRI With Random Encoding[J]. IEEE Transactions on Medical Imaging, 2011, 30(4): 893–903.
- [9] R. Otazo, D. Kim, L. Axel, and D. K. Sodickson, Combination of compressed sensing and parallel imaging for highly accelerated first-pass cardiac perfusion MRI[J]. Magnetic Resonance in Medicine, 2010, 64(3): 767–776.
- [10] B. Zhao, J. P. Haldar, C. Brinegar, and Z. P. Liang. In Proceedings of the 7th IEEE International Symposium on Biomedical Imaging: From Nano to Macro, Netherlands, 2010[C]. Rotterdam, A A balkerma ,2010.
- [11] XU Bin, TANG Yuanyan, FANG Bin. Image texture features classification based on Shearlet transform[J], Computer Engineering and Applications, 2011, 47(29):15-18.
- [12] GUO K, LABATE D. Optimally sparse multidimensional representation using Shearlets[J]. SIAM J Math Anal, 2007, 39:298-318.
- [13] EASLEY G, LIM W, LABATE D. Sparse directional image representations using the discrete Shearlet transform[J]. Appl Comput Harmon Anal, 2008, 25:25-46.
- [14] HU Haizhi, SUN Hui, etc. Image de-noising algorithm based on Shearlet transform[J], JOURNAL OF COMPUTER APPLICATIONS, 2010, 30(6):1562 -1564.
- [15] She Qingshan, Xu Ping, etc. A new image reconstruction algorithm of block compressed sensing[J], Journal of Southeast University (Natural Science Edition), 2011, 41:27-31.
- [16] TROPP J A, GILBERT A C. Signal recovery from random measurements via orthogonal matching pursuit[J]. IEEE Transactions on Information Theory, 2007, 53(12):4655-4666.
- [17] Guo Qiang. study of image statistical model based on shear waves transformation and its application[D], Shanghai University, Shanghai, China, 2010.
- [18] Zamani, M., Abdul Manaf, A., Abdullah, S., & Shojae Chaeikar, S. (2012). Mazdak Technique for PSNR Estimation in Audio Steganography Applied Mechanics and Materials (Vol. 229, pp. 2798-2803): Trans Tech Publications Inc.
- [19] Zamani, M., Abdul Manaf, A., & Daruis, R. (2012). Azizah Technique for Efficiency Measurement in Steganography. Paper presented at the 8th International Conference on Information Science and Digital Content Technology, Jeju.